Journal of Fluids and Structures (1997) **11,** 73–87

IN-LINE RESPONSE OF A HORIZONTAL CYLINDER IN REGULAR AND RANDOM WAVES

Y. S. Li, S. Zhan and S. L. Lau

Department of Civil and Structural Engineering, The Hong Kong Polytechnic University, Hung Hom, Kowloon, Hong Hong

(Received 22 April 1995 and in revised form 29 July 1996)

The in-line response of a horizontal flexibly mounted cylinder in regular and random waves are reported in this paper. Both theoretical analyses and experimental measurements have been carried out. The theoretical predictions are based on the Morison equation which is solved by the incremental harmonic balance method. The relationship between the response of the cylinder and the ratio of natural frequency of the cylinder to the wave frequency is first determined. Experiments are then performed in a wave flume to determine the accuracy of the Morison equation in predicting the in-line response of the cylinder in regular and in random waves. It has been verified that the Morison equation is valid under regular waves. For random waves, it is found that the in-line response can be predicted accurately by a superposition of the response to wave components of different frequencies using the Morison equation, only when the ratio of wave height to cylinder diameter is small.

1. INTRODUCTION

The prediction of the response of a flexibly mounted circular cylinder in wavy flows is a difficult problem due to the complexity of the fluid–structure interaction mechanisms. The study of the response of a circular cylinder in steady flows and oscillatory flows has attracted much attention, and the dynamics is now fairly well understood, a coherent account of which can be found in various textbooks and review papers [see, for example, Sarpkaya & Isaacson (1981) and Blevins (1990)]. However, investigations in the response of a cylinder in waves where water particle velocity varies with water depth are still scarce. In this paper, the study of the in-line response of a horizontal cylinder to both regular and random waves is reported. Both theoretical analyses and experimental measurements have been carried out. The theoretical predictions are based on the Morison equation which is solved by the incremental harmonic balance (IHB) method [see, for example, Lau & Cheung (1981) and Lau & Zhang (1992)]. The incremental harmonic balance method is very effective for solving nonlinear dynamic problems. The response (the horizontal displacement of the cylinder in this case) is represented by a Fourier series and all the Fourier coefficients are computed. Hence, the relationship between resonance and the frequency ratio, ω_n/ω, where ω_n is the natural angular frequency of the cylinder and ω is the angular frequency of the wave, can be easily identified.

Williamson (1985) investigated the validity of using the Morison equation for nonstationary structures by comparing predictions with results from experimental measurements. He reported that the forces on an elastically mounted horizontal cylinder and its in-line response in the sinusoidal flow of a U-tube showed good

0889–9746/97/010073 + 15 $25.00/fl960067

agreement with predictions. Lipsett & Williamson (1994) studied the two-dimensional response of a flexibly mounted horizontal rigid cylinder submerged in one arm of a U-tube. The conclusion is that simple mathematical models based on the Morison equation are able to predict the cylinder response in a satisfactory fashion, even though the interaction between the response of the cylinder and the flow is very complicated. Borthwick & Herbert (1988) measured the forces and responses of a spring-mounted vertical cylinder in regular waves generated in a laboratory flume. They also used the Morison equation to predict the in-line loading and response of the cylinder, and they found responses with frequencies at odd multiples of the wave frequency, in addition to the dominant component at the wave frequency. Sumer *et al.* (1989) reviewed the results of a model test study to determine the hydroelastic vibrations of a marine pipeline placed in the vicinity of a scoured trench and exposed to regular and irregular waves. They observed that the in-line movement of the pipe was generally larger for irregular waves. Falco *et al.* (1991) investigated the effects of regular waves on a horizontal submerged cylinder oscillating freely in the vertical direction. The conclusions are that the Morison equation, with coefficients obtained in the case of waves, fits the experimental results for the first harmonic well, but for the case of $\omega_n/\omega = 2$, the peak of the cylinder response appears in the cylinder natural frequency while the component at the wave frequency is negligible.

The main objective of the present study is to investigate the possible extension of the Morison equation for predicting the response of elastically mounted structures to both regular and random waves. The in-line response of a flexibly mounted horizontal cylinder placed in a wave flume is measured and compared with theoretical predictions based on the Morison equation. Since it is revealed in the theoretical analysis that superharmonic resonance occurs at $\omega_n/\omega = 3$, a transfer function relating the random wave spectrum to the cylinder response spectrum can be found only when the ratio of wave height to cylinder diameter is small. The experimental results of the present study confirm that when such a condition is satisfied, the response of the cylinder in random waves can be predicted accurately using the Morison equation, by simply superposing the responses to different wave components.

2. MATHEMATICAL MODELLING

The equation used to describe the in-line response of an oscillating horizontal circular cylinder in waves is the Morison equation which can be written as follows, taking into account the effect of the wave-induced orbital motions (Chaplin 1985; Faltinsen 1990):

$$M\ddot{x} + c\dot{x} + k_s x = \tfrac{1}{2}\rho D L C_D (u - \dot{x})\sqrt{(u - \dot{x})^2 + w^2} + C_M \frac{\rho \pi D^2 L}{4}\dot{u}, \tag{1}$$

where M is the mass of cylinder plus the added mass $= m + C_a \rho \pi D^2 L/4$, ρ the fluid density, D the cylinder diameter, and L the length of the cylinder; C_a is the added mass coefficient, c the structural damping of cylinder system, k_s the effective spring stiffness, C_D the drag coefficient, and C_M the inertia coefficient; x is the cylinder displacement, u the horizontal velocity component of fluid particles, and w the vertical velocity component of fluid particles. The overdot in equation (1) represents differentiation with respect to t.

The ratio of L/D used in the experiments to be described later is about 18 and hence end effects can be neglected. The horizontal and vertical fluid velocities u and w, at

location z (measured upwards from the still water level) under a small amplitude wave of amplitude $\frac{1}{2}H$, angular frequency ω, wave number k and water depth d are given by

$$u = \frac{gHk}{2\omega}\frac{\cosh k(d+z)}{\cosh kd}\cos \omega t, \qquad w = -\frac{gHk}{2\omega}\frac{\sinh k(d+z)}{\cosh kd}\sin \omega t, \tag{2}$$

where g is the gravitational acceleration.

Equation (1) can be written in the following form:

$$\omega^2\ddot{x} + \gamma\omega\dot{x} + \omega_n^2 x - \alpha(u - \omega\dot{x})\sqrt{(u-\omega\dot{x})^2 + w^2} + \beta \sin \tau = 0, \tag{3}$$

where

$$\gamma = c/M; \qquad \omega_n^2 = k_s/M;$$

$$\alpha = \frac{\rho D L C_D}{2M}; \qquad \beta = \frac{C_M \rho \pi D^2 L g H k \cosh k(d+z)}{8M \cosh kd}; \qquad \tau = \omega t;$$

and differentiation now is with respect to τ instead of t.

For simplicity, equation (3) is rewritten in the compact form:

$$F(\ddot{x}, \dot{x}, x, \tau) = 0. \tag{4}$$

Equation (4) is solved by the IHB (incremental harmonic balance) method. Let x_0 be an approximate solution and $x_0 + \Delta x_0$ be a more accurate solution to equation (4). Then, using the Taylor series expansion, we have

$$F(\ddot{x}_0, \dot{x}_0, x_0, \tau) + \frac{\partial F}{\partial \ddot{x}_0}\Delta\ddot{x}_0 + \frac{\partial F}{\partial \dot{x}_0}\Delta\dot{x}_0 + \frac{\partial F}{\partial x_0}\Delta x_0 = 0 \tag{5}$$

with

$$\frac{\partial F}{\partial \ddot{x}_0} = \omega^2,$$

$$\frac{\partial F}{\partial \dot{x}_0} = \gamma\omega + \alpha\omega\sqrt{(u-\omega\dot{x}_0)^2 + w^2} + \frac{\alpha\omega(u - \dot{\omega}x_0^2)}{\sqrt{(u-\omega\dot{x}_0)^2 + w^2}},$$

and

$$\frac{\partial F}{\partial x_0} = \omega_n^2.$$

Representing x_0 by a Fourier series,

$$x_0 = a_0 + \sum_{n=1}^{N}(a_n \cos n\tau + b_n \sin n\tau), \tag{6a}$$

then we have

$$\dot{x}_0 = \sum_{n=1}^{N}(-na_n \sin n\tau + nb_n \cos n\tau), \tag{6b}$$

$$\ddot{x}_0 = \sum_{n=1}^{N}(-n^2 a_n \cos n\tau - n^2 b_n \sin n\tau), \tag{6c}$$

and

$$\Delta x_0 = \Delta a_0 + \sum_{n=1}^{N}(\Delta a_n \cos n\tau + \Delta b_n \sin n\tau). \tag{6d}$$

After substituting equations (6a) to (6d) in equation (5), we have

$$\frac{\partial F}{\partial \ddot{x}_0}\left[\sum_{n=1}^{N} -n^2(\Delta a_n \cos n\tau + \Delta b_n \sin n\tau)\right] + \frac{\partial F}{\partial \dot{x}_0}\left[\sum_{n=1}^{N} (-n\,\Delta a_n \sin n\tau + n\,\Delta b \cos n\tau)\right]$$
$$+ \frac{\partial F}{\partial x_0}\left[\Delta a_0 + \sum_{n=1}^{N} (\Delta a_n \cos n\tau + \Delta b_n \sin n\tau)\right] = -F(\ddot{x}_0, \dot{x}_0, x_0, \tau), \quad (7)$$

or

$$\frac{\partial F}{\partial x_0}\Delta a_0 + \sum_{n=1}^{N}\left(\frac{\partial F}{\partial x_0}\cos n\tau - \frac{\partial F}{\partial \dot{x}_0} n \sin n\tau - \frac{\partial F}{\partial \ddot{x}_0} n^2 \cos n\tau\right)\Delta a_n$$
$$+ \sum_{n=1}^{N}\left(\frac{\partial F}{\partial x_0}\sin n\tau + \frac{\partial F}{\partial \dot{x}_0} n \cos n\tau - \frac{\partial F}{\partial \ddot{x}_0} n^2 \sin n\tau\right)\Delta b_n = -F(\ddot{x}_0, \dot{x}_0, x_0, \tau). \quad (8)$$

Applying the Galerkin method, i.e., multiplying equation (8) in turn by 1, $\cos\tau$, $\cos 2\tau, \ldots, \sin N\tau$, and integrating with respect to τ between the limits of 0 and 2π, a set of $(2N+1)$ equations for the unknown coefficients $\Delta a_0, \Delta a_1, \Delta a_2, \ldots, \Delta b_N$ can be found. Hence, a better solution, $x_0 + \Delta x_0$, is obtained from the initial approximate solution, x_0. The computation of the Fourier coefficients of $\dfrac{\partial F}{\partial \dot{x}_0}$ can be facilitated by using the Fast Fourier Transform. The procedure is repeated a number of times until a solution of desired accuracy is obtained. In the present calculation, the iteration is stopped when the following criterion is satisfied:

$$\left|\frac{\max(\Delta a_0, \Delta a_1, \ldots, \Delta b_N)}{\max(a_0, a_1, \ldots, b_N)}\right| < 10^{-8}. \quad (9)$$

It is found that the IHB method is very effective for solving equation (5), and any reasonable initial trial solution x_0 would converge rapidly to the true solution.

The numerical solution of equation (1) can be simplified by the linearization of the drag term as given by Malhotra & Penzien (1970) resulting in the following approximate equation of motion (the effect of the vertical fluid velocity is also neglected):

$$M\ddot{x} + (c + \tfrac{1}{2}\rho D L C_D \sqrt{8/\pi}\sigma_r)\dot{x} + k_s x = \tfrac{1}{2}\rho D L C_D \sqrt{8/\pi}\sigma_r u + C_M \frac{\rho\pi D^2 L}{4}\dot{u}, \quad (10)$$

where

$$\sigma_r = \sqrt{\frac{(u_{\max} - b_1\omega)^2 + (a_1\omega)^2}{2}}.$$

Since σ_r is related to the unknown function x, equation (10) has again to be solved by iteration using the IHB method. However, the amount of computations is less than that required for solving equation (5). It can be seen from Figures 1 and 2 that the quasi-linear equation (10) can give a good solution to the problem. The values of the various parameters such as c, k_s, C_D and C_M adopted in equations (1) and (10) to give Figures 1 and 2 are the same as that of the experimental cylinder described later in

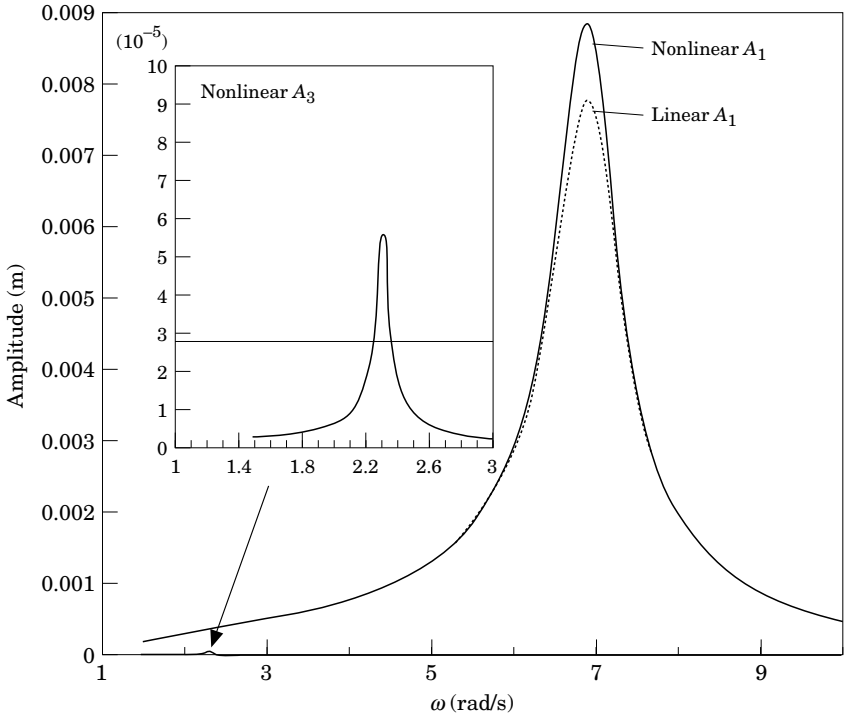

Figure 1. Comparison between quasi-linear and nonlinear solutions for $H/D = 0{\cdot}048$. $H = 0{\cdot}004$ m, D = cylinder diameter; $A_1(=\sqrt{a_1^2 + b_1^2})$ = amplitude of 1st harmonic, and $A_3(=\sqrt{a_3^2 + b_3^2})$ = amplitude of 3rd harmonic.

Section 3. In this paper, all theoretical solutions are obtained from solution of the nonlinear equation of motion (1), unless explicitly stated to the contrary.

3. MEASUREMENT OF IN-LINE OSCILLATION

3.1. Measurement of Parameters c, k_s, C_D and C_M

The experimental set-up is shown schematically in Figure 3. The cylinder used in the study of the in-line response is made from a plastic tube with an outside diameter of 82·6 mm and a length of 1·45 m. The cylinder is positioned horizontally, with its centre at a distance 0·195 m below the water surface, in a 1·5 m wide wave flume, by a vertical steel plate having a cross-section of 100 mm × 10 mm at each of its two ends. The steel plates are in turn fixed at their upper ends to a steel I-beam above the wave flume.

The sensors are located between the cylinder and the vertical steel plates and can be either very stiff for measurement of wave forces on a fixed cylinder or elastic for measurement of in-line responses to wave motions. The transverse movement is suppressed. The sensors are a pair of stainless steel plates with waterproof strain gauges fixed to them for deflection measurement. The stainless steel plates for the in-line force sensors are shorter and thicker than that for the displacement sensors to provide the necessary stiffness. The wave motion is measured by wave height gauges. The wave probe of the wave-height gauge consists of a pair of stainless steel rods which are immersed to such a depth that they are always in contact with the water surface

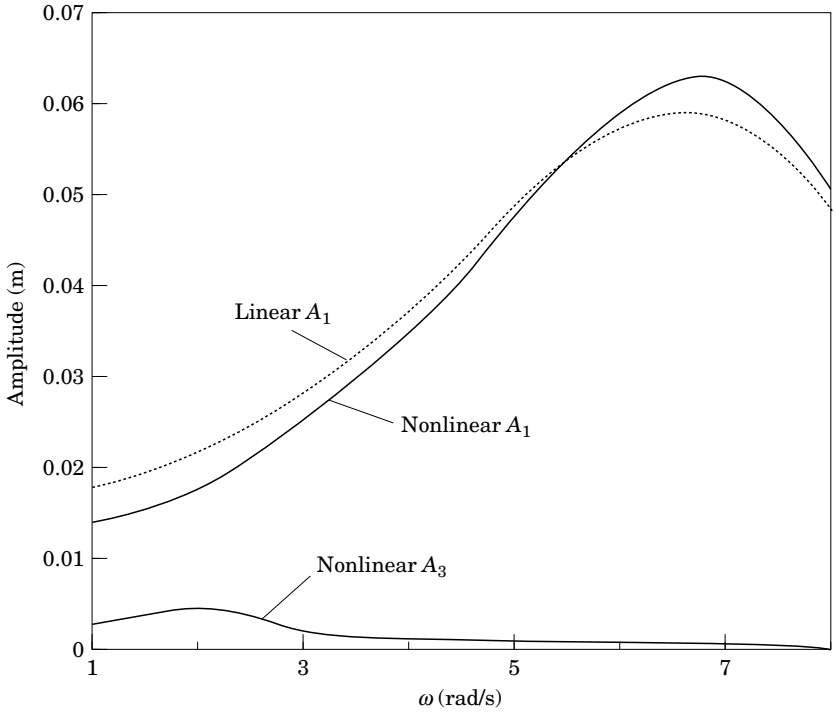

Figure 2. Comparison between quasi-linear and nonlinear solutions for $H/D = 1{\cdot}816$. $H = 0{\cdot}15$ m, D = cylinder diameter; $A_1(=\sqrt{a_1^2 + b_1^2})$ = amplitude of 1st harmonic, and $A_3(=\sqrt{a_3^2 + b_3^2})$ = amplitude of 3rd harmonic.

under wave measuring conditions. The mass of the cylinder is $m = 7{\cdot}13$ kg. The structural damping c and spring stiffness k are first determined by allowing the cylinder to oscillate freely in air. The time history of the free oscillation is shown in Figure 4. From this time history, it is found that $c = 1{\cdot}8$ N s/m and $k_s = 851$ N/m.

The drag coefficient, C_D, is then determined by allowing the cylinder to oscillate freely in still water. The time history of one such oscillation is shown in Figure 5. It is found that the natural frequency of the cylinder $\omega_n = 6{\cdot}9$ rad/s and $M = k_s/\omega_n^2 = 17{\cdot}85$ kg. The drag coefficient then is obtained from the following expression:

$$C_D = \frac{3T_d c\left(\dfrac{A_0}{A'} - \exp\left(\dfrac{cT_d}{4M}\right)\right)}{8\rho DLA_0\left(\exp\left(\dfrac{cT_d}{4M}\right) - 1\right)} = 2{\cdot}65, \tag{11}$$

where A_0 is the initial displacement of cylinder (i.e. at $t = 0$), A' the displacement of cylinder at $t = \frac{1}{2}T_d$, and T_d is the period of oscillation in still water.

The derivation of equation (11) is given in the Appendix. It has been assumed that both c and k_s are the same in air and water. Reynolds number and the Keulegan–Carpenter number corresponding to the maximum velocity of the cylinder in the first half cycle of oscillation are 3290 and 0·38, respectively. This method of determining C_D is more accurate than the commonly used method of measuring wave forces, because the drag force is very small for small values of the ratio of wave height to cylinder diameter, as is the case in the present series of experiments ($H/D \approx 1/20$). The value of C_D thus determined can be used later to determine the response of the cylinder in

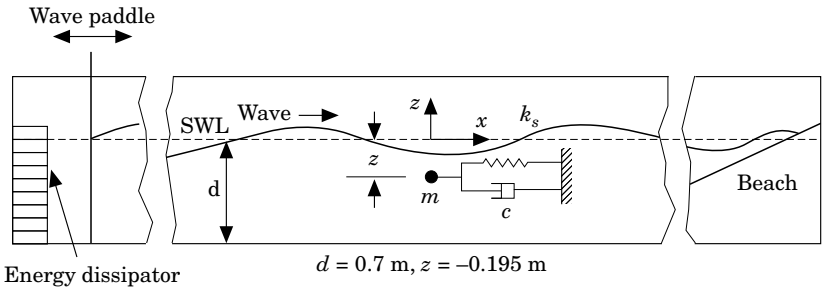

(a) Submerged cylinder in wave flume

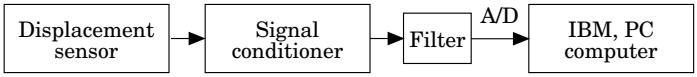

(b) Measurement of c and C_D

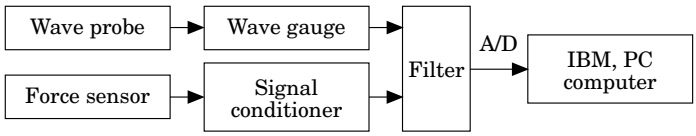

(c) Measurement of C_M

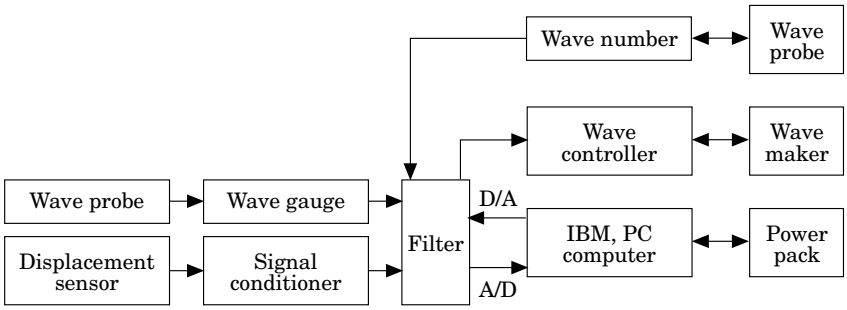

(d) Measurement of oscillations

Figure 3. Experimental set-up.

waves, because the Reynolds number under which C_D is determined is close to that of the wave experiments.

The inertia coefficient, C_M, was determined by measuring the in-line force, F_x, on the cylinder due to regular waves. Williamson (1985) showed that for an elastically mounted cylinder in an oscillatory flow, the values of C_D and C_M are not significantly removed from that of the fixed cylinder, except near resonance ($\omega/\omega_n \simeq 1$), and advised that the change in the coefficients due to the response of the structure should be taken into account near resonance. Hence errors in the prediction of cylinder response are expected near resonance if C_M is measured for a fixed cylinder in waves. The experimental results are shown in Figure 6. The following expression based on the

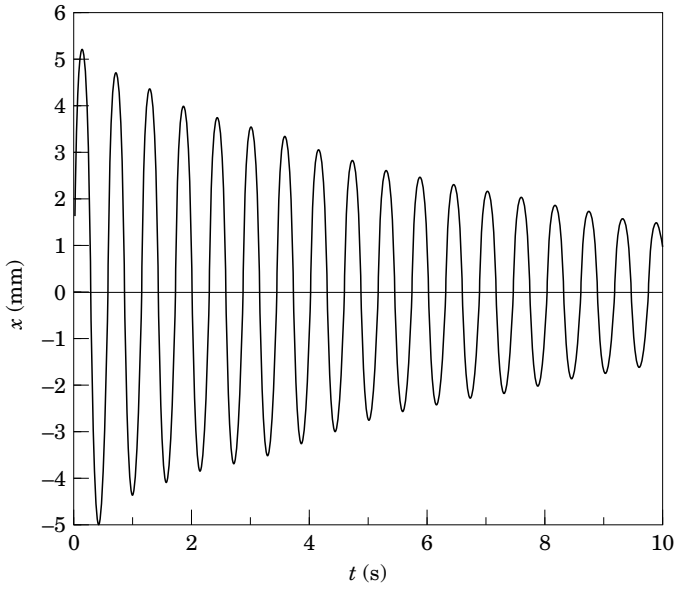

Figure 4. A record of free vibration in air.

Fourier averaging technique over one cycle [see, for example, Chakrabarti (1987)] is used for the calculation of C_M:

$$C_M = -\frac{\dfrac{2}{T}\displaystyle\int_0^T F_x \sin \omega t \, \mathrm{d}t}{\rho \dfrac{\pi D^2 L}{4} \dfrac{gHk}{2} \dfrac{\cosh k(d+z)}{\cosh kd}}. \tag{12}$$

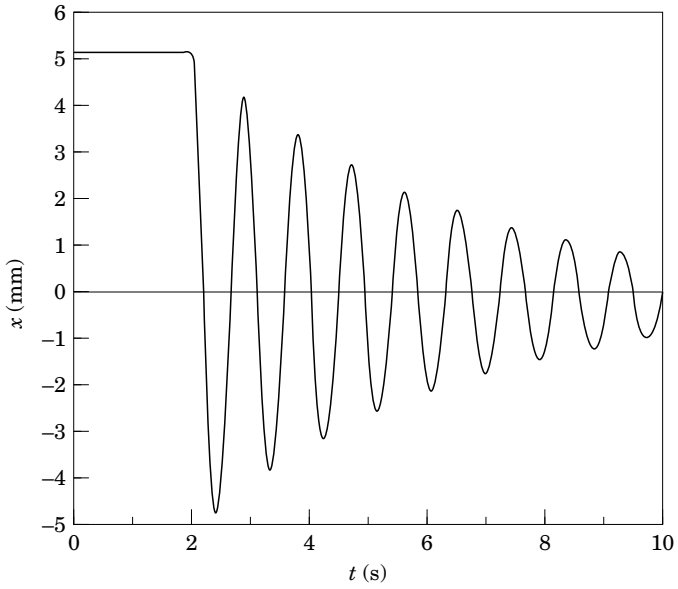

Figure 5. A record of free vibration in water.

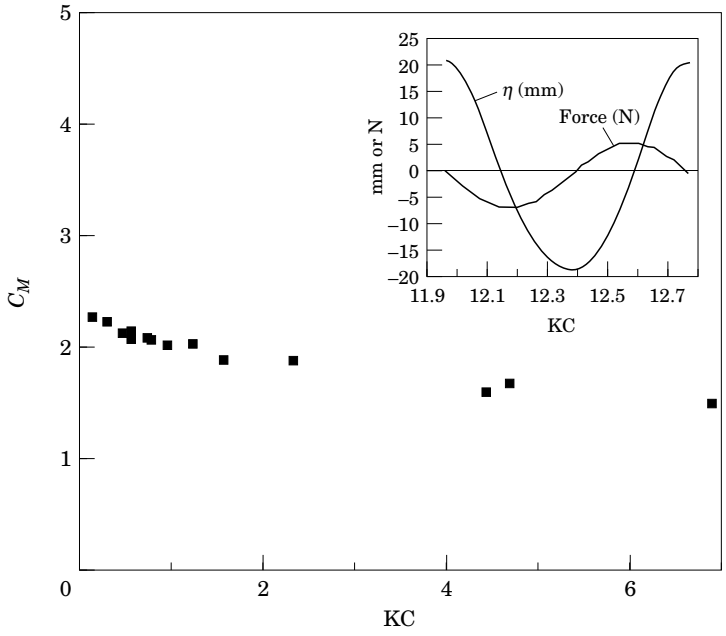

Figure 6. Variation of C_M with the Keulegan–Carpenter number.

In the response computations described below, the value of C_M is taken as 2·1.

3.2. Response of Cylinder in Regular and Random Waves

Both the computed and experimental results for the amplitudes $A_1(=\sqrt{a_1^2+b_1^2})$ of the response at excitation frequency in regular waves at a wave height of 0·004 m are shown in Figure 7. (Theoretical values of A_3 are shown in Figure 1.) It is observed that the computed values agree very well with the experimental results. The cylinder primarily oscillates at the same frequency as the water waves and resonance occurs at the natural frequency of the cylinder $\omega_n = 6{\cdot}9$ rad/s. The amplitude of the response of the cylinder at resonance is about 2·2 times the wave height. Except when ω is in the vicinity of $\frac{1}{3}\omega_n$, the other Fourier coefficients of the cylinder response are very small, about two orders of magnitude smaller than A_1. At $\omega = \frac{1}{3}\omega_n$, the amplitude of the third harmonic, $A_3(=\sqrt{a_3^2+b_3^2})$, is about $A_1/5$ and a record of the oscillation of the cylinder at this frequency is shown in Figure 8 to illustrate this superharmonic resonance.

The response of the cylinder in random waves has also been investigated using the JONSWAP spectrum. Typical records of the input random wave, the resulting dynamic response of the cylinder and the response spectrum, as well as the spectrum of the free surface elevation η, are shown in Figures 9, 10 and 11, respectively. The input random wave shown in Figure 9 corresponds to the following wind conditions: fetch = 5 km; wind speed = 1 m/s and model scale = 1. The details for the transformation of wind speed and fetch into spectrum parameters can be found in Houmb & Overvik (1976). The theoretical spectra of cylinder displacement, $G_x(f)$, are synthesized from computed responses in regular waves of different frequencies, assuming the existence of a transfer function $H(f)$, i.e. $G_x(f) = |H(f)|^2\, G_\eta(f)$, where $G_\eta(f)$ is the wave spectrum.

It is known from the theoretical analysis of the system under regular waves that, when the ratio of $H/D = 0{\cdot}048$, the amplitude of the third harmonic, A_3, is only about

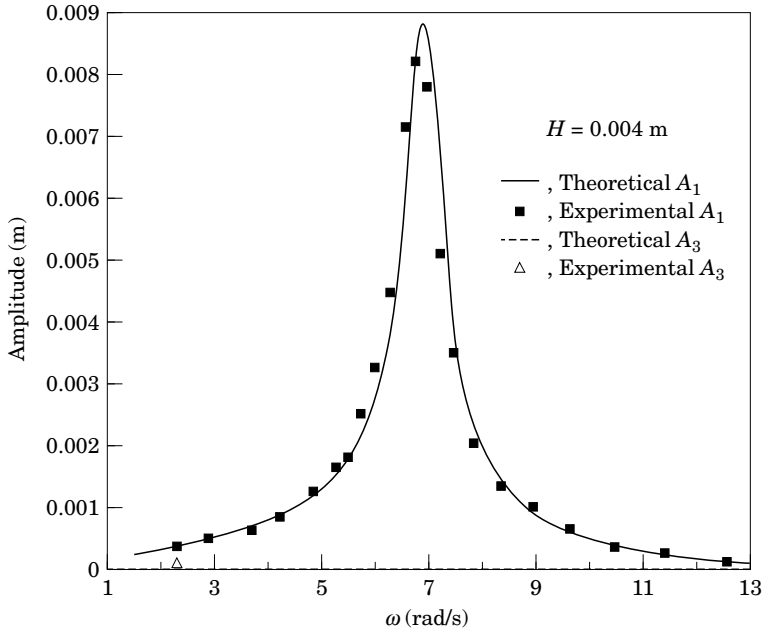

Figure 7. Comparison between theory and experiment; $H = 0{\cdot}004$ m.

1/5 of A_1 even at superharmonic resonance, $f = \frac{1}{3}f_n$, and hence A_3^2 is at most 4% of A_1^2. Furthermore, the value of A_3 at $\frac{1}{3}f_n$ is only about 1/120 of A_1 at f_n, and the corresponding ratio of the square of the amplitudes is about 1/14 400. Thus if the ratio of H/D is small, the nonlinear effects are weak and the response of the cylinder to random wave excitation can simply be obtained by superposing the contributions from individual wave components, as described below.

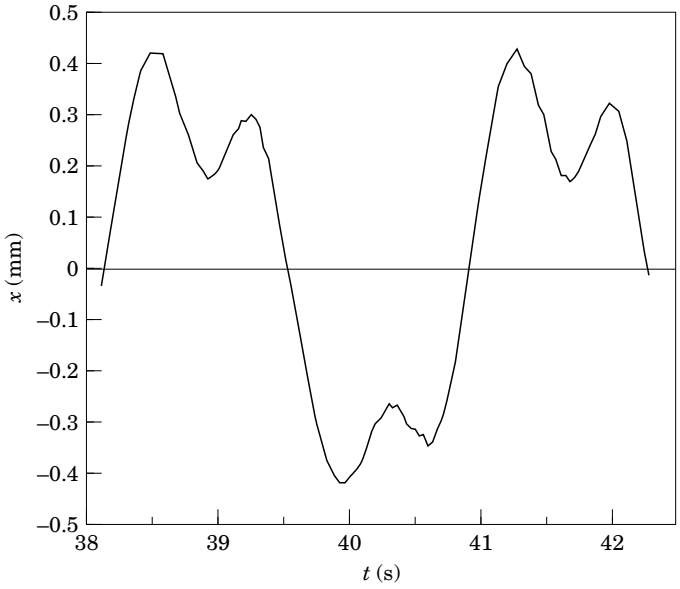

Figure 8. A record showing triple-frequency harmonic resonance.

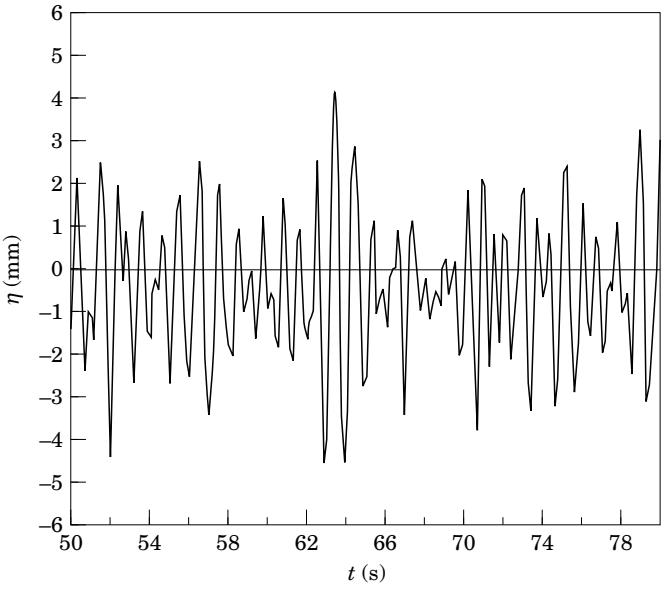

Figure 9. A record of random waves.

Firstly, the surface elevation, η, is expressed as

$$\eta = \sum_{i=1}^{n} \frac{H_i}{2} \cos(k_i x - \omega_i t + \phi_i). \tag{13}$$

The amplitudes of the first harmonic A_{1i} of the dynamic response corresponding to each wave component are calculated by solving equation (1) using the IHB method. The spectrum of the dynamic response of the cylinder is then given by

$$G_x(f_i) = \frac{A_{1i}^2}{2\,\Delta f}, \tag{14}$$

where Δf is the chosen frequency-band size.

It can be seen from Figure 11 that the calculated spectrum based on superposition of individual wave components agrees well with the measured spectrum, except that the calculated peak is higher than the corresponding measured peak. For higher H/D ratios, the nonlinear effect cannot be neglected due to an increase of the amplitude of the third harmonic A_3, and hence the method of superposition cannot be used. Similarly, Figure 12 gives the spectra of the cylinder response and the free surface elevation for the case of fetch = 10 km, wind speed = 2·5 m/s and model scale = 9. The calculated and measured spectra also match well.

4. CONCLUSIONS

In the range of Keulegan–Carpenter number investigated here (KC $<$ 7), the present study confirms the validity of the Morison equation for predicting the in-line response of a flexibly mounted horizontal cylinder in regular waves. The theoretical predictions of the cylinder response obtained by solving the Morison equation using the incremental harmonic balance method agree well with experimental measurements.

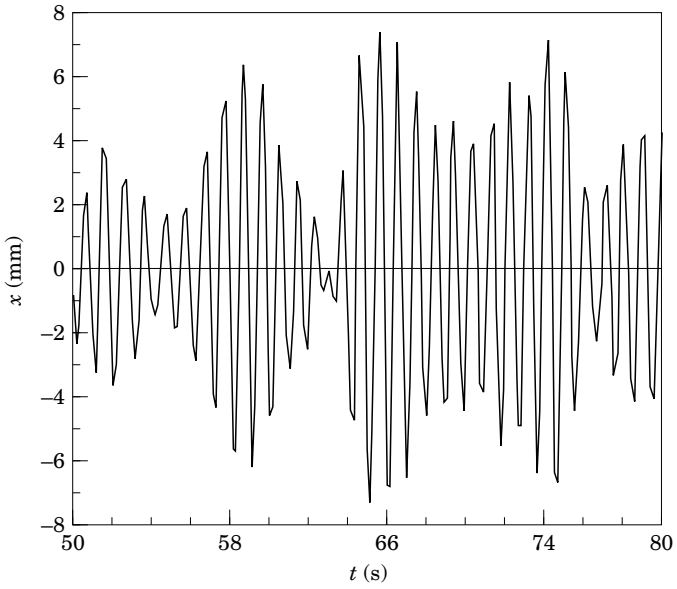

Figure 10. A record of dynamic response in random waves.

Because of the occurrence of superharmonic resonance at $\omega_n/\omega = 3$, the in-line response in random waves can be predicted using the Morison equation by a superposition of the responses to different wave components only when the ratio of wave height to cylinder diameter is small. The possibility of using the Morison equation for the prediction of two-dimensional responses requires further investigation, due to the complex interaction between oscillations in-line and transverse with the velocity vector.

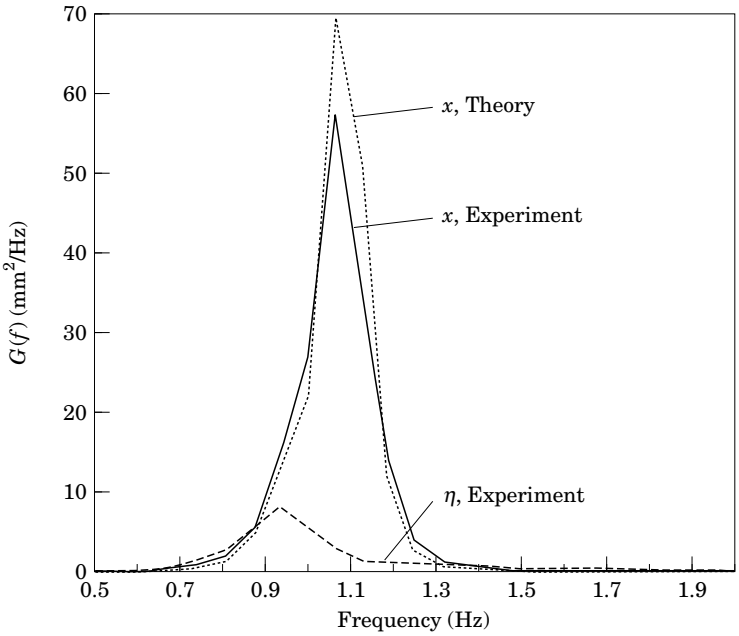

Figure 11. Wave and resulting response spectra I.

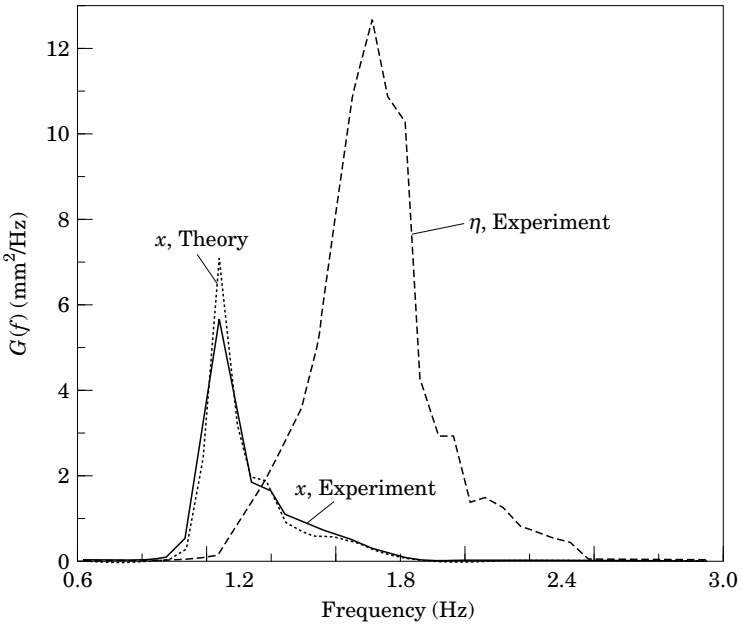

Figure 12. Wave and resulting response spectra II.

ACKNOWLEDGEMENTS

This work was supported by a research grant (No. 340/681) from the Hong Kong Polytechnic University and was performed while the second author was on leave from the Department of Mechanics and Engineering at Zhongshan University, People's Republic of China.

REFERENCES

BLEVINS, R. D. 1990 *Flow-Induced Vibration,* 2nd ed. New York: Van Nostrand Reinhold.

BORTHWICK, A. G. L. & HERBERT, D. M. 1988 Loading and response of a small diameter flexibly mounted cylinder in waves. *Journal of Fluids and Structures* **2,** 479–501.

CHAKRABARTI, S. K. 1987 *Hydrodynamics of Offshore Structures.* Berlin: Springer-Verlag.

CHAPLIN, J. R. 1985 Morison inertia coefficients in orbital flow. *ASCE Journal of Waterway, Port, Coastal and Ocean Engineering* **111,** 201–215.

FALCO, M., MIMMI, G. & TANZI, E. 1991 Dynamic actions due to wave motion on horizontal submerged cylinders oscillating in vertical direction. In *Proceedings of the Institution of Mechanical Engineers Conference on Flow Induced Vibration,* pp. 93–99, Brighton, U.K. London: I. Mech. E.

FALTINSEN, O. M. 1990 *Sea Loads on Ships and Offshore Structures.* Cambridge: Cambridge University Press.

HOUMB, O. G. & OVERVIK, T. 1976 Parameterization of wave spectra and long term distribution of height and period. In *Proceedings of Conference on Behaviour of Offshore Structures,* pp. 144–169, Trondheim, Norway.

LAU, S. L. & CHEUNG, Y. K. 1981 Amplitude incremental variational principle for nonlinear vibratrion of elastic system. *Journal of Applied Mechanics* **48,** 959–964.

LAU, S. L. & ZHANG, W.-S. 1992 Nonlinear vibrations of piecewise-linear systems by incremental harmonic balance method. *Journal of Applied Mechanics* **59,** 153–160.

LIPSETT, A. W. & WILLIAMSON, I. D. 1994 Response of a cylinder in oscillatory flow. *Journal of Fluids and Structures* **8,** 681–709.

MALHOTRA, A. K. & PENZIEN, J. 1970 Non-deterministric analysis of offshore structures. *ASCE Journal of Engineering Mechanics Division* **96,** 985–1003.

SARPKAYA, T. & ISAACSON, M. 1981 *Mechanics of Wave Forces on Offshore Structures.* New York: Van Nostrand Reinhold.

SUMER, B. M., FREDSØE, J., GRAVESEN, H. & BRUSCHI, R. 1989 Response of marine pipelines in scour trenches. *ASCE Journal of Waterway, Port, Coastal and Ocean Engineering* **115,** 477–496.

WILLIAMSON, C. H. K. 1985 In-line response of a cylinder in oscillatory flow. *Applied Ocean Research* **7,** 97–106.

APPENDIX

The derivation of equation (11) starts with the following equation of motion:

$$M\ddot{x} + c\dot{x} + k_s x = -\tfrac{1}{2}\rho D L C_D\,|\dot{x}|\,\dot{x}, \tag{A1}$$

or

$$\ddot{x} + \omega_n^2 x = -\gamma(\dot{x} + \alpha\,|\dot{x}|\,\dot{x}), \tag{A2}$$

where

$$\gamma = c/M, \qquad \alpha = \tfrac{1}{2}\rho D L C_D/c, \quad \text{and} \quad \omega_n^2 = k_s/M.$$

Let the solution of equation (A2) be

$$x = A(t)\cos[\omega_n t + \phi(t)], \tag{A3}$$

then

$$\dot{x} = \dot{A}\cos[\omega_n t + \phi] - A\omega_n \sin[\omega_n t + \phi] - A\dot{\phi}\sin[\omega_n t + \phi]. \tag{A4}$$

Because the nonlinear vibrarion is weak, both $\dot{A}$ and $\dot{\phi}$ are small with respect to A since they vary very slowly with time; therefore, we can let

$$\dot{A}\cos[\omega_n t + \phi] - A\dot{\phi}\sin[\omega_n t + \phi] = 0. \tag{A5}$$

Hence,

$$\dot{x} = -A\omega_n \sin[\omega_n t + \phi], \tag{A6}$$

$$\ddot{x} = -\dot{A}\omega_n \sin[\omega_n t + \phi] - A\omega_n^2 \cos[\omega_n t + \phi] - A\omega_n\dot{\phi}\cos[\omega_n t + \phi]. \tag{A7}$$

Substituting equation (A3), (A6) and (A7) into equation (A2), yields

$$-\dot{A}\omega_n \sin\psi - A\dot{\phi}\omega_n \cos\psi = \gamma(A\omega_n \sin\psi + \alpha A^2\omega_n^2\,|\sin\psi|\sin\psi), \tag{A8}$$

where $\psi = \omega_n t + \phi$.

From equations (A5) and (A8), we find

$$\dot{A} = -\gamma(A\sin\psi + \alpha A^2\omega_n\,|\sin\psi|\sin\psi)\sin\psi. \tag{A9}$$

It is difficult to find an analytical solution for equation (A9). An approximate solution is found by taking

$$\begin{aligned}\dot{A} &= -\frac{\gamma}{2\pi}\int_0^{2\pi}(A\sin\psi + \alpha A^2\omega_n\,|\sin\psi|\sin\psi)\sin\psi\,\mathrm{d}\psi \\ &= -\frac{\gamma}{2}A - \frac{4\gamma\alpha\omega_n}{3\pi}A^2.\end{aligned} \tag{A10}$$

Integrating equation (A10) and using the initial condition $A = A_0$ at $t = 0$, gives

$$A = \frac{\gamma A_0}{\left(\gamma + \dfrac{8A_0\gamma\alpha\omega_n}{3\pi}\right)\mathrm{e}^{\gamma t/2} - \dfrac{8A_0\gamma\alpha\omega_n}{3\pi}}. \tag{A11}$$

If $A = A'$ at $t = \frac{1}{2}T_d$, then we have

$$\alpha = \frac{3T_d\left(\frac{A_0}{A'} - e^{\gamma T_d/4}\right)}{16A_0(e^{\gamma T_d/4} - 1)},$$

or

$$C_D = \frac{3T_d c\left(\frac{A_0}{A'} - \exp\left(\frac{cT_d}{4M}\right)\right)}{8\rho DLA_0\left(\exp\left(\frac{cT_d}{4M}\right) - 1\right)}. \tag{A12}$$